

# Advanced simulations on laser annealing: explosive crystallization and phonon transport corrections

Alberto Sciuto

Dipartimento di Fisica e Astronomia  
Ettore Majorana  
Università di Catania  
Via S. Sofia 64, 95123 Catania, Italy  
and CNR IMM  
Z.I. VIII Strada 5, 95121 Catania, Italy  
Email: alberto.sciuto@imm.cnr.it

Ioannis Deretzis,  
Giuseppe Fisicaro,  
Salvatore F. Lombardo,  
Antonino La Magna

CNR IMM  
Z.I. VIII Strada 5, 95121 Catania, Italy

Maria Grazia Grimaldi

Dipartimento di Fisica e Astronomia  
Ettore Majorana  
Università di Catania  
Via S. Sofia 64, 95123 Catania, Italy

Karim Huet,  
Bobby Lespinasse,  
Armand Verstraete,  
Benoit Curvers

LASSE  
laser systems and solutions of Europe  
14-38 Rue Alexandre, 92230 Gennevilleres, France

Igor Bejenari,  
Alexander Burenkov,  
Peter Pichler

Fraunhofer IISB  
Schottkystrasse 10, 91058 Erlangen, Germany

**Abstract**—Current semiconductor device manufacturing often needs the integration of annealing process steps with a low thermal budget; and, among them, pulsed laser annealing (LA) is a reliable option. Consequently, the use of LA specialized Technology Computer Aided Design (TCAD) models is emerging as a support for the development of this particular heating methods. Anyway, models already implemented in academic or commercial packages usually consider some approximations which can lead to inaccurate predictions if they are applied in rather common configurations of nano-device: i.e. structures with  $nm$  wide elements where amorphous pockets are also present. In particular, in these cases non-diffusive thermal transport and explosive crystallization could take place. Here we present upgrades of the LA TCAD models allowing the simulation of these phenomena. We will demonstrate that these models can be reliably integrated in the current TCAD packages discussing the key features of the numerical solutions features in some particular cases.

## I. INTRODUCTION

Thermal annealing with low thermal budget is nowadays a common processing step in the semiconductor device manufacturing. Laser annealing (LA), in particular, can be integrated in the process flow for micro-and nano-electronics, yielding versatile and powerful solutions in extremely constrained space and time scales. However, optimal control is a key

The research leading to these results has received funding from the European Union's Horizon 2020 research and innovation programme under grant agreement No. 871813 MUNDEFAB.

issue for the successful application of LA [1], [2] and, within this context, reliable simulations of LA processes are required for optimizing the process parameters while reducing the number of experimental tests. Despite LA models have been already implemented in academic or commercial packages, a further evolution of the methods is necessary for the general application in complex structures with  $nm$  wide elements, where the thermal transport is strongly limited by phonon effects. Moreover, due to the frequent presence of amorphous pockets in processed device structures, ultra-fast (explosive) amorphous-to-crystal phase transitions occurring during the irradiation of the devices could present a further challenging objective for LA modelling and simulation.

In this context, we integrate phonon transport corrections [3] and explosive crystallization models [4] to our existing simulation tool, LIAB (LASSE Innovation Application Booster) [5], which allow for reproducing experimental data while predicting the behavior of semiconductor structures upon laser annealing. We have simulated thermal transport induced by either conventional and laser annealing in various structures, comparing the results in which standard conditions and corrections of the Fourier law were applied. We demonstrate that corrections due to the finite phonon mean free paths can be suitably included in annealing process simulations of three-dimensional nanosystems. Moreover, the reliability of the corrections has been verified comparing continuous solutions

and Molecular Dynamic simulations in equivalent systems and heating conditions [6]. Finally we will demonstrate that the implementation in LIAB of a three phase mode 1 [4] allows accurate numerical solutions of the explosive crystallization phenomena in structured samples, therefore the impact of this phenomenon in the processing of nano-device can be potentially predicted.

## II. PHONONIC CORRECTION TO THERMAL TRANSPORT

A possible approach for the TCAD of a laser annealing process in systems with very small structures is the preliminary investigation based on Molecular Dynamics or Boltzmann Transport Equation of the analysed structure and the use of the estimated dependence of  $k_{app}(T)$  in the Time dependent Fourier Law.

$$C(T) \frac{\partial T}{\partial t} = \nabla \cdot [k_{bulk}(T) \nabla T] + S_T(t) \quad (1)$$

where  $C(T)$  is the thermal capacitance,  $k_{bulk}(T)$  the bulk thermal conductivity and  $S_T(t)$  is the time dependent internal heat source which implicitly depends on the T field.

However, this procedure is computationally expensive and practically unfeasible for general applications. An alternative method has been treated in the case of LA simulation in [3]. This method is consistent with the general result that the temperature field is ruled by Eq. 1 with the bulk value of the conductivity  $k_{bulk}(T)$  whilst corrections due to the finite phonon mean free path have to be considered only for the boundary conditions. In particular, using jump-lick BCs, exact solutions in the diffusive  $\langle Kn \rangle \ll 1$  and ballistic  $\langle Kn \rangle \gg 1$  limit can be obtained, while the solutions deviate only by a few percent with respect to the BTE solution in the intermediate  $\langle Kn \rangle \sim 1$  region. In this formalism, Dirichlet boundary conditions for a system in contact with a thermostat at a  $T_0$  is substituted by

$$\hat{n} \cdot \vec{F}_Q = k_{bulk} \lambda^{-1} (T - T_0) \quad (2)$$

Where  $\vec{F}_Q = \vec{F}_Q^+ - \vec{F}_Q^-$  is the combined phonon flux coming from the left and right size of the junction between the nano-system and the thermostat,  $k_{bulk}$  is the bulk thermal conductivity of the material and  $\lambda$  is the average phonon scattering length, which can be related to known and measurable material properties as

$$\lambda(T) = 4k_{bulk}(T)/C(T)v_s(T) \quad (3)$$

Moreover, the material boundary is ruled by the jump condition

$$-k_{bulk}^1 \nabla T_1 = \hat{\Pi} (T_1|_{\Gamma}^+ \hat{n}_1 + T_2|_{\Gamma}^- \hat{n}_2) \quad (4)$$

for the temperatures  $T_1$  and  $T_2$  at the interface  $\Gamma$  between two regions made of different materials. In Eq. 4  $\hat{n}_1 = -\hat{n}_2$  are the local outward normal unit vectors to the two sides of the boundary and  $\hat{\Pi} = (k_{bulk}^1 \lambda_1^{-1} + k_{bulk}^2 \lambda_2^{-1})|_{\Gamma}$  is the local phonon scattering functional. Moreover, the energy conservation condition at the boundary has to be imposed as:

$$-k_{bulk}^1 \nabla T_1|_{\Gamma} = -k_{bulk}^2 \nabla T_2|_{\Gamma} \quad (5)$$

Eq. 5 acts as a closure of the model at the interface location. We note that an external boundary simulating a virtual interface with the same material is still ruled by the Neumann relation  $\nabla T = 0$ .

The reliability of the approach can be demonstrated by calculating the apparent conductivity  $k_{app}$  which can be directly compared with MD estimates or experimental data [3]. According to Ref. [7]  $k_{app}$  can be calculated by:

$$k_{app}(T) = k_{bulk}(T) \frac{\langle T_{standard} - T_0 \rangle}{\langle T_{corrected} - T_0 \rangle} \quad (6)$$

where  $T_{correct}$  and  $T_{standard}$  are the corrected and diffusive temperature fields evaluated numerically, the symbol  $T_0$  is the thermostat temperature while  $\langle \rangle$  indicates the average of the field expression over the space region occupied by the structures.

As an example of the corrections' impact, we consider a Si nanowire (NW) having an almost regular polygon with 12 edges, in contact with one or two thermostats along one or two perimeter edges, while internally heated by a uniform source. In Fig. 1(a) we report a cross section perpendicular to the Si NW axis, of the thermal field obtained for the standard Dirichlet BC(s) (left side) and the corrected BC(s) expression (right side) for the edge(s) in contact with the thermostat. The temperature obtained in the two cases along the NW diameter connecting the center of the thermostat edge and the opposite edge is shown in Fig. 1(b). The difference between the standard and the corrected solution is relevant for this structure and it tends to enlarge (decrease) for smaller (larger) NWs.

The  $k_{app}(T)$  value estimated with the formula 6 for the NW with a diameter of 56nm is  $k_{app}(300K) = 21.5[W/mK]$ , for the thermal contact configuration of fig. 1, which is in nice agreement with the experimental measurement of ref. [8].  $k_{app}(T)$  reduces monotonically with the NW diameter; e.g. its value for T=300K and a NW of a 5.2 nm is in the range  $k_{app} \sim 1-2[W/mK]$ , in dependence of the contact realization. These values agree with MD estimates for NW of same size.

After the integration of the corrected boundary conditions in the LIAB package we can simulate the full LA process. Our computational code [5] uses the FEniCS (<https://fenicsproject.org/>) computing platform for solving the evolution of continuum fields and the Gmsh (<http://gmsh.info/>) library as a 3D finite element mesh generator.

As an example, we have investigated the laser thermal treatment of a 56 nm wide infinite Ge nanowire on a Si substrate. The presence in the device structures of interface between crystalline and amorphous materials needs a proper "ad-hoc" calibration for the interface boundary expression since the average phonon scattering length cannot be properly estimated by means of material properties in the amorphous phase. A ubiquitous example is the interface between the structure and the air. In the modeling of the process we introduced a scattering length  $\lambda_{air}$  to represent the air side of the interface between the studied system and the air portion itself. Fig. 2(a) shows the heat source distribution deriving

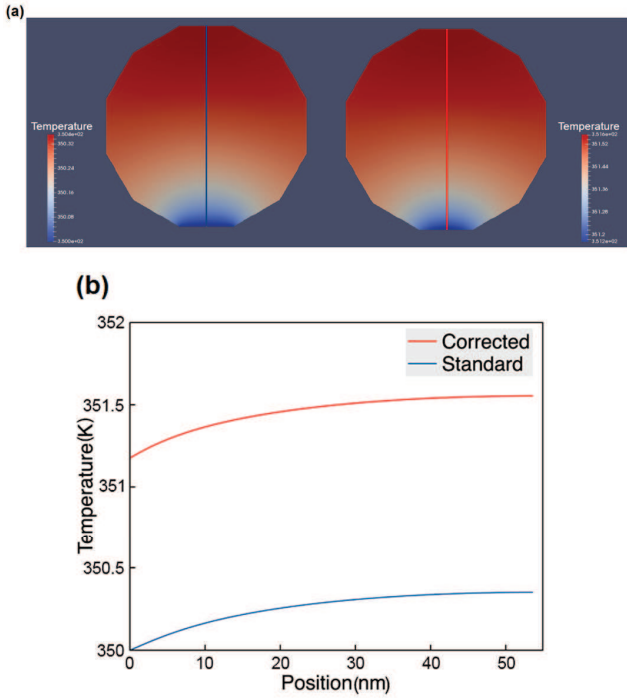


Fig. 1. (a) Cross section of a heated Si nanowire with a diameter of 56 nm: standard (left) and corrected (right) solutions. (b) Standard and corrected T values along the nanowire diameter line shown in (a). The correction is implemented as jump-like (i.e. Robin type) boundary condition in the Finite Elements Methods used to solve the heat equation. The discontinuity at the device/thermostat interface reproduces the incomplete thermalization of the internal phonon modes due to the nanosize of the system.

from the absorption of a laser pulse of  $\sim 160ns$  width and wave length of  $308nm$  after 5 ns heating for a value of the scattering length of  $\lambda_{air} = 3$  nm. Using these computed source distribution we simulated the heating using corrected and standard boundary conditions. The role of  $\lambda_{air}$  parameter is shown in Fig. 3 where the temperature profiles for different values of  $\lambda_{air}$  are plotted. A strong confinement is simulated for values of the scattering length similar to the ones derived in crystal material (red line) while the  $\lambda_{air} = 3nm$  one gives a smoother and more correct behavior. A further analysis of corrected versus standard solutions can be seen in Fig. 2(b), where the effect of heat confinement is more evident. We notice that the setting of the interface parameters for crystal-amorphous boundary is a critical issue of the method and deserves of further studies also with the aid of MD simulations.

### III. EXPLOSIVE CRYSTALLIZATION

Annealing processes of amorphous materials are rather usual in device technology and in most of the cases the crystal phase is recovered at the end of the process. In the case of LA application, the process can easily lead to a complex ultra fast phenomenon known as explosive crystallization. The Explosive Crystallization (EC) mechanism in covalent elemental semiconductors (Si and Ge) is the result of a significant larger (negative) latent heat for the liquid to crystal phase transition

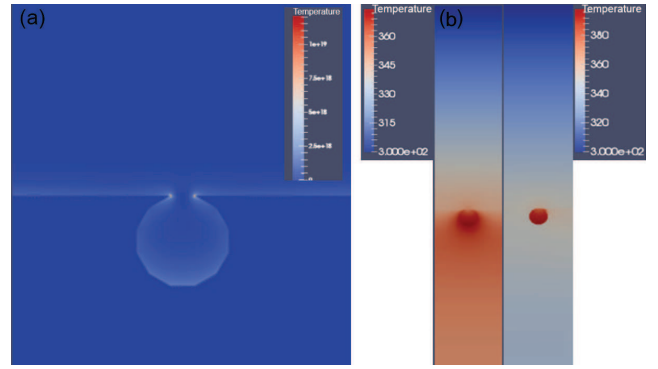


Fig. 2. (a) Source distribution simulated by LIAB after 5 ns heating with  $\lambda_{air} = 3$  nm, (b) Comparison between the results of the pulsed LA heating process after 30 ns from pulse starting instant with  $\lambda_{air} = 3$  nm with (right) and without (left) the corrections

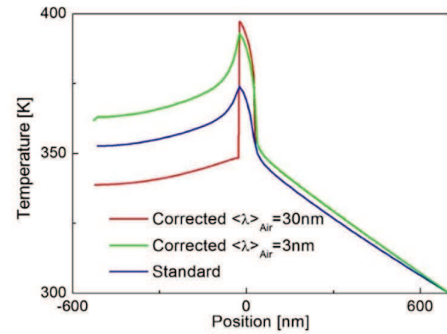


Fig. 3. Temperature profiles of 30 ns heating with different values of  $\lambda_{air}$ .

with respect to the one (positive) for the amorphous to liquid transition. The explosive kinetics of the process has to be naturally recovered by the model since there is the unbalance of the thermodynamic parameters of the three simultaneous phases.

The quantitative modeling of the EC phenomenon should allow the computation of the kinetics of both the crystal-liquid and liquid-amorphous front on the basis of the thermodynamic parameters of the materials in study. In ref. [4] a new method for the tracking of the interface is proposed. The formalism is a natural extension of the phase field one that we normally use to study melting and ensures an efficient computational way to solve a multiple phase problem. The new formulation relies on the presence of three local minima of the potential energy density at  $-1, 0, 1$  (in contrast with the two minima of the classical phase field Wheeler's formulation [9] that represent, respectively, the amorphous, liquid and crystal phase. All the physical parameters (including the ones ruling the dopant evolution) in this approach must interpolate the calibrated values in the three phases. As an example, heat capacity, one of the parameters of the model that clearly depends on temperature and phase, behaves in this particular way:

## CONCLUSIONS

$$C(\phi, T) = \theta(\phi) C_c(T) + [1 - \theta(\phi)] C_a(T) + C_l(T) [1 - |\phi|] \quad (7)$$

where  $\theta(\phi)$  is the Heaviside step function while the  $c$ ,  $a$ ,  $l$  subscripts indicate crystal, amorphous and liquid phases respectively.

We have moreover successfully simulated this challenging behavior that includes secondary melting during the process. Fig. 4 shows a 2D melting front driven by an ultrafast re-crystallization in a simple Si slab with a 50 nm narrowing of the structure, in order to test the robustness of the solution with hard edges.

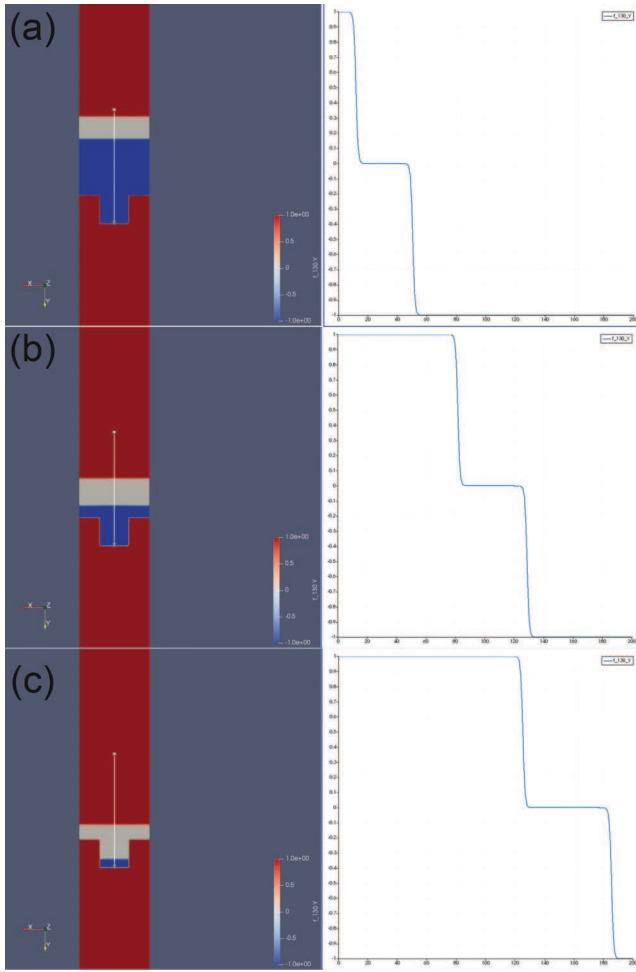


Fig. 4. Snapshots of 2D explosive crystallization at (a) 78 ns (b) 84 ns and (c) 89 ns. The red, blue and grey regions are crystal, amorphous and liquid, respectively. The initial thickness of the amorphous region is indicated by the vertical line, whilst the top region in red is filled by air. The lateral dimension of the structure is 50 nm and periodic boundary conditions are applied along the  $x$ -axis.

This work focuses on two crucial, industry standard driven, aspects of the current advancements in LA simulations. A more refined control on thermal transport is key to correctly simulate the behaviour of Laser Annealing, especially in smaller structures, where geometry and size plays an important role. The failure of classical heat transport in these structures opens the possibility to explore new ways of accounting for phonon driven effects without the need of solving directly transport equations for the particles, the method that we proposed, as we have seen is, in fact, less resource demanding and can be easier to implement with the current state of the art TCAD tools. Another crucial aspect that we implemented in our simulation code is explosive crystallization. The possibility to investigate this ultrafast phenomenon is key to a better understanding and control of advanced processes especially when accounting for dopant diffusion and alloy behaviour. For this purpose, we have implemented a multi-well phase-field model specifically suited for the simulation of explosive crystallization induced by pulsed laser irradiation in the nanosecond time scale. The numerical implementation of the model is robust despite the discontinuous jumps of the interface speed induced by the phenomenon.

## REFERENCES

- [1] S. F. Lombardo, S. Boninelli, F. Cristiano, G. Fiscaro, G. Fortunato, M. G. Grimaldi, G. Impellizzeri, M. Italia, A. Marino, R. Milazzo, E. Napolitani, V. Privitera, and A. La Magna, "Laser annealing in Si and Ge: Anomalous physical aspects and modeling approaches," *MATERIALS SCIENCE IN SEMICONDUCTOR PROCESSING*, vol. 62, no. SI, pp. 80–91, MAY 2017.
- [2] K. Huet, J. Aubin, P. E. Raynal, B. Curvers, A. Verstraete, B. Lespinasse, F. Mazzamuto, A. Sciuto, S. F. Lombardo, A. La Magna, P. Acosta-Alba, L. Dagault, C. Licitra, J. M. Hartmann, and S. Kerdiles, "Pulsed laser annealing for advanced technology nodes: Modeling and calibration," *APPLIED SURFACE SCIENCE*, vol. 505, MAR 1 2020.
- [3] A. Sciuto, I. Deretzis, G. Fiscaro, S. F. Lombardo, M. G. Grimaldi, K. Huet, B. Curvers, B. Lespinasse, A. Verstraete, and A. La Magna, "Phononic transport and simulations of annealing processes in nanometric complex structures," *Physical Review Materials*, vol. 4, no. 5, p. 056007, 2020.
- [4] S. Lombardo, S. Boninelli, F. Cristiano, I. Deretzis, M. Grimaldi, K. Huet, E. Napolitani, and A. La Magna, "Phase field model of the nanoscale evolution during the explosive crystallization phenomenon," *Journal of Applied Physics*, vol. 123, no. 10, p. 105105, 2018.
- [5] S. Lombardo, G. Fiscaro, I. Deretzis, A. La Magna, B. Curver, B. Lespinasse, and K. Huet, "Theoretical study of the laser annealing process in finfet structures," *Applied Surface Science*, vol. 467, pp. 666–672, 2019.
- [6] A. Burenkov, V. Belko, and J. Lorenz, "Self-heating of nano-scale SOI MOSFETS: TCAD and molecular dynamics simulations," in *19<sup>th</sup> International Workshop on Thermal Investigations of ICs and Systems (THERMINIC)*. IEEE, 2013, pp. 305–308. [Online]. Available: 10.1109/THERMINIC.2013.6675230
- [7] J. Kaiser, T. Feng, J. Maassen, X. Wang, X. Ruan, and M. Lundstrom, "Thermal transport at the nanoscale: A fourier's law vs. phonon boltzmann equation study," *Journal of Applied Physics*, vol. 121, no. 4, p. 044302, 2017. [Online]. Available: <https://doi.org/10.1063/1.4974872>
- [8] J. Anaya, J. Jimenez, and T. Rodriguez, "Thermal transport in semiconductor nanowires," in *Nanowires*, X. Peng, Ed. Rijeka: IntechOpen, 2012, ch. 11. [Online]. Available: <https://doi.org/10.5772/52588>
- [9] A. A. Wheeler, W. J. Boettinger, and G. B. McFadden, "Phase-field model for isothermal phase transitions in binary alloys," *Phys. Rev. A*, vol. 45, pp. 7424–7439, May 1992. [Online]. Available: <http://link.aps.org/doi/10.1103/PhysRevA.45.7424>